Algorithm Theoretical Basis Document (ATBD) of Vegetation Indices and Vegetation Fraction Retrieval from OCM-3 payload onboard Oceansat-3

Document Version 2.0

Mehul R. Pandya

AED, BPSG, EPSA

Space Applications Centre, Ahmedabad

January 2021

ATBD: Vegetation Indices

1.0 Algorithm Specifications:

Version	Date	Prepared by	Description
1.0	15/01/2021	Dr. Mehul R. Pandya and Dr. Vishal N. Pathak	ATBD of Vegetation Indices and Vegetation Fraction retrieval from OCM-3 payload on-board Oceansat-3

2.0 Introduction

The use of Ocean Color Monitor (OCM-3) data for land product algorithms such as vegetation indices, vegetation fraction, albedo, leaf area index etc would make OCM-3 an ideal platform for global vegetation monitoring.

The OCM-3 vegetation indices (VIs) and vegetation fraction will provide consistent, spatial and temporal fields of global vegetation conditions that will be used to monitor the Earth's terrestrial photosynthetic vegetation activity for phenologic, change detection, and biophysical derivation of radiometric and structural vegetation parameters. The OCM-3 vegetation index (VI) products will play a major role in several Earth observation studies as well as be an integral part in the production of many global and regional biospheric models and biogeochemical cycles. Satellite-derived vegetation indices are being integrated in interactive biosphere models as part of global climate modelling (Sellers et al. 1994; Raich and Schlesinger, 1992; Fung et al., 1987; Tans et al., 1990) and production efficiency models (Prince et al., 1994; Prince, 1991). They are also used in a wide variety of land applications, including natural resource management, agriculture, hydrology monitoring and modeling etc.

The OCM-3 instrument contains specifications, which will help make an improved Normalized Difference Vegetation Index (NDVI), Vegetation Fraction (VF) and Enhanced Vegetation Index (EVI). Most important is the availability of 13 channels in the spectral interval spanning from 0.407 to 1.020 µm. Therefore, we one can derive exact NDVI, VF and EVI.

This Algorithm Theoretical Basis Document (ATBD) describes the algorithm that will be used to retrieve Normalized Difference Vegetation Index (NDVI), Vegetation Fraction (VF) and Enhanced Vegetation Index (EVI) from ISRO's planned mission, Oceansat-3 (OS-3). To retrieve NDVI, VF and EVI at regular interval, observations in blue, red and near infrared bands will be used from OS-3 Ocean Colour Monitor (OCM-3). The output NDVI, VF and EVI product description is summarized in Table 1.

Table 1: Summary of Vegetation Indices products

Parameter Name	Units	Horizontal Cell Size	Comments
Normalized Difference Vegetation Index (NDVI)	Dimensionless	360 m	Retrieved for all cloud free pixels.
Enhanced Vegetation Index (EVI)	Dimensionless	360 m	Retrieved for all cloud free pixels.
Vegetation Fraction	Dimensionless	360 m	Retrieved for all cloud free pixels.

This document describes the instrument characteristics, input data, both OCM-3 and other data required for retrieval of NDVI, VF and EVI along with theoretical background for usage of these datasets; details of inputs and output data; implementation flow and also provides assumptions and limitations of proposed algorithm.

3.0 OCM-3 Specifications

Ocean Color Monitor 3 (OCM-3) will have 13 spectral bands in the region of 0.407 to 1.020 µm. The instrument specifications for OCM-3 are shown in table-2 and 3.

Table-2: OCM-3 Sensor Specifications

Parameter	Value
IGFOV (m)	360
Total lens assemblies and DHA	13
Pixel size and pitch (µm)	10
Detector format (pixels)	4000 x 48
Focal length (mm)	20
F-number	4.3/4.5
Field-of-view (˚)	±43.5
Integration time	53.46 ms
Transmission bits	12
SNR at reference radiance	> 1000 for B1 to B10 > 800 for B11 to B13

Table-3: OCM-3 Band description and their applications

Band No.	Central Wavelength	Application
B1	412 nm	Differentiate yellow substance from chlorophyll
B2	443 nm	Chlorophyll absorption maximum; low chlorophyll
B3	490 nm	Moderate chlorophyll
B4	510 nm	High chlorophyll; Total Suspended Matter (TSM)
B5	555 nm	Weak chlorophyll absorption
B6	566 nm	Phycoerythrobilins (PEB)
B7	620 nm	Turbidity in coastal Case 2 waters
B8	670 nm	Baseline for chlorophyll fluorescence
B9	681 nm	Chlorophyll fluorescence for high concentration
B10	710 nm	Baseline for chlorophyll fluorescence; extrapolation to visible bands for atmospheric Correction
B11	780 nm	Atmospheric correction; avoids O2 absorption Band
B12	870 nm	Atmospheric correction; good assessment of spectral scattering
B13	1010 nm	Atmospheric correction, aerosol – white foam discrimination

4.0 Theoretical basis for the Vegetation indices

Many studies have shown the relationships of red and near-infrared (NIR) reflected energy to the amount of vegetation present on the ground (Colwell, 1974). Reflected red energy decreases with plant development due to chlorophyll absorption within actively photosynthetic leaves. Reflected NIR energy, on the other hand, will increase with plant development through scattering processes (reflection and transmission) in healthy, turgid leaves. Unfortunately, because the amount of red and NIR radiation reflected from a plant canopy and reaching a satellite sensor varies with solar irradiance, atmospheric conditions, canopy background, and canopy structure/ and composition, one cannot use a simple measure of reflected energy to quantify plant biophysical parameters nor monitor vegetation on a global, operational basis. This is made difficult due to the intricate radiant transfer processes at both the leaf level (cell

constituents, leaf morphology) and canopy level (leaf elements, orientation, nonphotosynthetic vegetation (NPV), and background). This problem has been circumvented somewhat by combining two or more bands into an equation or 'vegetation index' (VI). The simple ratio (SR) was the first index to be used (Jordan, 1969), formed by dividing the NIR response by the corresponding 'red' band output,

$$SR = \frac{X_{nir}}{X_{red}} \qquad (1)$$

where X can be digital counts, at- satellite radiances, top of the atmosphere apparent reflectances, land leaving surface radiances, surface reflectances, or hemispherical spectral albedos. However, for densely vegetated areas, the amount of red light reflected approaches very small values and this ratio, consequently, increases without bounds. Deering (1978) normalized this ratio from -1 to +1, with the normalized difference vegetation index (NDVI), by ratioing the difference between the NIR and red bands by their sum;

$$NDVI = \frac{X_{nir} - X_{red}}{X_{nir} + X_{red}} \qquad (2)$$

For terrestrial vegetation targets the lower boundary generally becomes approximately 0.15 and the upper boundary approximately 0.95.

Global-based operational applications of the NDVI have utilized digital counts, at-sensor radiances, 'normalized' reflectances (top of the atmosphere), partially atmospheric corrected (ozone absorption and molecular scattering) reflectances or surface reflectance (atmospherically corrected reflectance). Thus, the NDVI has evolved with improvements in measurement inputs. In the absence of atmospheric correction procedure, most of the times, top of the atmosphere reflectance or a partial atmospheric correction for Rayleigh scattering and ozone absorption is used operationally for the generation of the Advanced Very High Resolution Radiometer; Agbu et al., 1994, (AVHRR) Pathfinder and the IGBP Global 1km NDVI data sets (James and Kalluri 1994; Townshend et al. 1994). The NDVI is currently the only operational, global-based vegetation index utilized. This is in part, due to its 'ratioing' properties, which enable the NDVI to cancel out a large proportion of signal variations attributed to calibration, noise, and changing irradiance conditions that accompany changing sun angles, topography, clouds/shadow and atmospheric conditions.

As a vegetation monitoring tool, the NDVI is utilized to construct seasonal, temporal profiles of vegetation activity enabling interannual comparisons of these profiles. The temporal profile of the NDVI has been shown to depict seasonal and phenologic activity, length of the growing season, peak greenness, onset of greenness, and leaf turnover or 'dry-down' period. Myneni et al. (1997) presented a 10 year NDVI data record of northern Boreal forests showing a warming trend whereby the length of the growing season had increased by nearly 2 weeks. They showed the usefulness of such NDVI growing season plots for change detection and monitoring. Tucker (1985) similarly used NDVI seasonal profiles to show desert expansions and contractions in the Sahara. The time integral of the NDVI over the growing season has been correlated with net primary production (NPP) (Running and Nemani, 1988; Prince, 1991; Justice et al., 1985; Goward et al., 1991, Tucker and Sellers, 1986).

VIs and VF play an important role in climatic, hydrologic, and geochemical and VF is widely used to describe vegetation quality and ecosystem change. It is also a controlling factor in transpiration, photosynthesis, global climate changes and other terrestrial processes and climate models. The VF can be derived from NDVI using following equation.

$$Vegetation\ Fraction\ (VF) = \frac{NDVI_i - NDVI_{min}}{NDVI_{max} - NDVI_{min}} \qquad (3)$$

Where, $NDVI_{min}$ and $NDVI_{max}$ are the signals from bare soil and dense green vegetation, respectively. And $NDVI_i$ represents NDVI value of individual pixel.

Many studies have shown the NDVI to be related to leaf area index (LAI), green biomass, percent green cover, and fraction of absorbed photosynthetically active radiation (fAPAR) (Asrar et al., 1984; Baret and Guyot, 1991; Goward and Huemmrich, 1992; Sellers, 1985; Sellers, 1986; Running and Nemani, 1988; Tucker et al., 1981; Curran, 1980). Relationships between fAPAR and NDVI have been shown to be near linear (Pinter, 1993; Begué, 1993; Wiegand et al., 1991; Daughtry et al., 1992), in contrast to the non-linearity experienced in LAI – NDVI relationships with saturation problems at LAI values over 2. Other studies have shown the NDVI to be related to carbon-fixation, canopy resistance, and potential evapotranspiration allowing its use as input to models of biogeochemical cycles (Raich and Schlesinger, 1992; Fung et al., 1987; Sellers, 1985; Asrar et al., 1984; Running et al., 1989; Running, 1990; IGBP, 1992).
Another newer index called the enhanced vegetation index (EVI) will be generated from the OCM-3 dataset. The EVI can be computed using the equation 4, which are shown in figure 2.

$$EVI = G\,X\,\frac{\rho_{NIR}-\rho_{Red}}{\rho_{NIR}+C1*\rho_{Red}-C2*\rho_{blue}+L} \qquad (4)$$

Where, L is the canopy background adjustment and C1, C2 are aerosol resistance terms L=1, C1=6, C2=7.5, G=2.5 (gain factor). The reflectance terms of three bands ($\rho_{blue}, \rho_{Red}, \rho_{NIR}$) may be taken as TOA reflectance or Rayleigh corrected reflectance.

5.0 Atmospheric effects

The atmosphere degrades the NDVI value by reducing the contrast between the red and NIR reflected signals. The red signal normally increases as a result of scattered, upwelling path radiance contributions from the atmosphere, while the NIR signal tends to decrease as a result of atmospheric attenuation associated with scattering and water vapor absorption. The net result is a drop in the NDVI signal and an underestimation of the amount of vegetation at the surface. The degradation in NDVI signal is dependent on the aerosol content of the atmosphere, with the turbid atmospheres resulting in the lowest NDVI signals. The impact of atmospheric effects on NDVI values is most serious with aerosol scattering (0.04 - 0.20 unit decreases), followed by water vapor (0.04 - 0.08), and Rayleigh scattering (0.02 - 0.04) (Goward et al. 1991; Teillet, 1989). The atmosphere problem may be corrected through direct and indirect means (Kaufman and Tanre, 1996). Atmospheric effects on the OCM-3 VI's may become minimal if the atmospheric correction algorithms being implemented prior to VI computation. Spatial variations in smoke, gaseous and particulate pollutants, and light cirrus clouds, may be present at the finer spatial resolutions. Kaufman and Tanré (1992) developed the atmospherically resistant vegetation index (ARVI) as an example of an indirect approach to atmosphere correction, utilizing the difference of the blue and red bands as an indicator of atmospheric noise. The ARVI accounts for atmosphere aerosol scattering and requires atmospheric correction of molecular scattering and ozone absorption prior to its use. Myneni and Asrar (1993), in a sensitivity study with simulated data, found the ARVI to reduce atmospheric effects and to mimic ground-based NDVI data. Pinty and Verstraete (1992) have proposed an AVHRR-specific, global environment monitoring index (GEMI), which minimizes atmospheric effects specific to AVHRR data sets. We propose to use the atmosphere resistance concept (blue/ red) in the enhanced VI (EVI) to aid with highly variable aerosol conditions, such as smoke from biomass burning. The NDVI and EVI from OCM-3 will be computed using the surface reflectance if they are available, otherwise top of the atmosphere (TOA) observations will be used in the present study to derive the vegetation indices.

6.0 Algorithm Description

Vegetation indices are empirical measures of vegetation activity. The primary goal is to formulate a precise measure of spatial/ temporal variations in vegetation while maintaining an equation that is robust and sensitive over a global range of vegetation conditions. The vegetation index equations presented here utilize the red and NIR reflected signals to isolate and enhance the 'green', photosynthetically-active vegetation component of a given pixel. The red and NIR responses are radiometrically calibrated, cloud-filtered, top-of-atmosphere (TOA) or atmospherically corrected (if available) and spatially and temporally gridded, to produce the vegetation index maps. In the following section the flowchart is provided (figure 1) and equations from which the VI products are derived are also presented briefly.

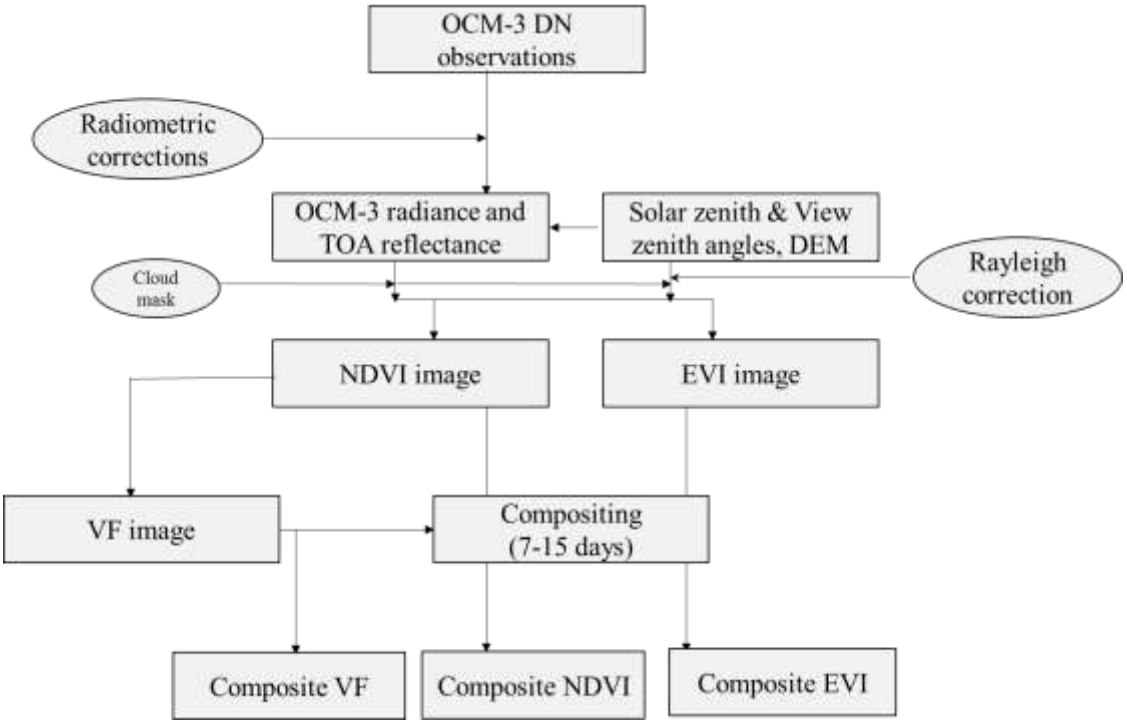

Figure 1. Flowchart showing generation of NDVI, VF and EVI products from OCM-3 observations

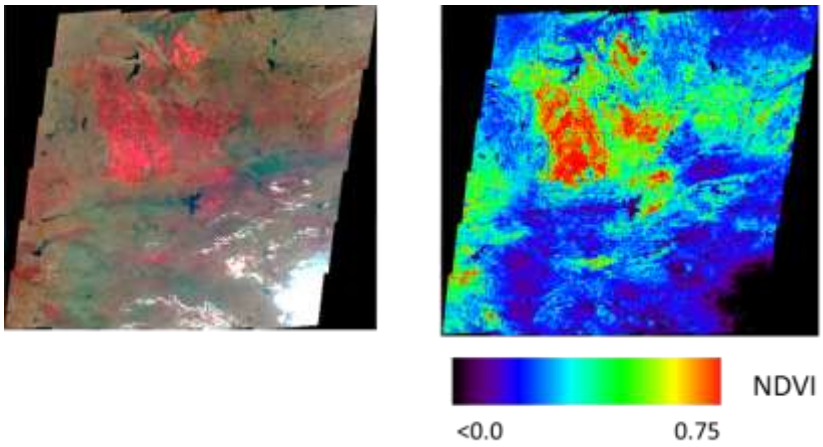

Figure 2. The normalized difference vegetation index (NDVI) computed using the GHRC red and NIR observations

As discussed in equation (2) NDVI will be derived using following equation 2 from TOA reflectance (or surface reflectance if available). An example of NDVI generated from the

GHRC observations is shown in figure 2. While, the enhanced vegetation index (EVI) will be generated from the OCM-3 dataset using equation 4, which is shown in figure 3.

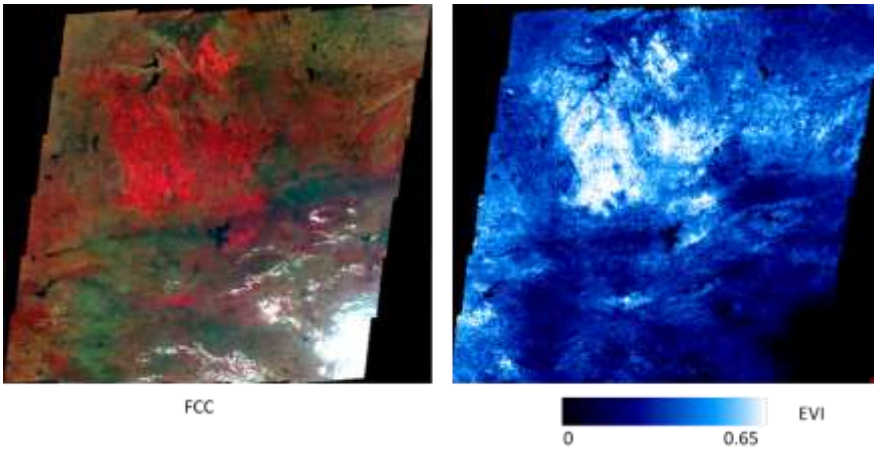

Figure 3. Enhanced vegetation index (EVI) computed using GHRC blue, red & NIR data

7.0 Data Inputs and Outputs

Inputs

Static data requirement

Parameter	Resolution	Source
Spectral Response Function (SRF) for OCM-3 bands	1nm	Sensor laboratory of Space Applications Centre, Ahmedabad

Image and pre-processing data (Dynamic)

Parameter	Resolution	Quantization	Accuracy	Source
Geometrically and radiometrically corrected TOA or Atmospherically corrected reflectances products for OCM-3 bands	360 m	---	SNR >400 @ 5% albedo & geolocation accuracy should be less than 0.5 of pixel resolution	Provided by DP and EPSA team engaged in geometric and surface reflectances generation
Cloud mask for each acquisition	All pixels	---	Not greater than 1 pixel	DP team
Sun and view angles of each pixel				DP team

Output data

Parameter	Unit	Min	Max	Accuracy	Resolution
Daily NDVI	Dimensionless	-1	+1	>95% (Targeted)	360 m
Daily VF	Dimensionless	0	+1	>95% (Targeted)	360 m
Daily EVI	Dimensionless	-1	+1	>95% (Targeted)	360 m
Composite NDVI (7 & 10-Day) (i) Fixed date composite (ii) Dynamic composite	Dimensionless	-1	+1	>95% (Targeted)	360 m
Composite VF (7 & 10-Day) (iii) Fixed date composite (iv) Dynamic composite	Dimensionless	0	+1	>95% (Targeted)	360 m
Composite EVI (7 & 10-Day) (v) Fixed date composite (vi) Dynamic composite	Dimensionless	-1	+1	>95% (Targeted)	360 m

8.0 Compositing and optimization of NDVI, VF & EVI

The construction of weekly, 10-day, seasonal or temporal profiles requires a separate 'compositing' algorithm in which several VI images, over a given time interval (7-days, 10-days, etc) are merged to create a single cloud-free image VI map with minimal atmospheric and sun-surface-sensor angular effects (Holben, 1986). Moderate and coarse resolution satellite systems, such as MODIS, the AVHRR, SPOT4-VEGETATION (Systeme Pour l'Observation de la Terre 4-VEGETATION; Archard et al., 1994), SeaWiFS (Sea-Viewing Wide Field-of-View Sensor; Hooker et al., 1994), and GLI (Global Imager; Nakajima et al., 1998) acquire global bi-directional radiance data of the Earth's surface under a wide variety of solar illumination angles, sensor view angles, atmospheres, and cloud conditions. The procedure generally used for generation of composited, NDVI products is the maximum value compositing (MVC) technique. This is accomplished by selecting, on a pixel by pixel basis, the input pixel with the highest NDVI value as output to the composited product. The procedure generally includes cloud screening and data quality checks (Goward et al., 1994; Eidenshink and Faundeer, 1994). Since residual cloud cover, not accounted for in the cloud masking procedure, and atmospheric sources of contamination both lower NDVI values, a maximum NDVI would select the least cloud- and atmospheric-contaminated pixels. Furthermore, since the influence of atmospheric contamination and residual cloud cover increases with optical path length, the maximum NDVI criterion also has a tendency to select the most near-nadir view and smallest solar zenith angle pixels (least optical path lengths), thus standardizing to a certain

degree the variable sun-surface-sensor observation geometries over a compositing cycle (Holben 1986; Cihlar et al. 1994a).

The MVC works nicely over near-Lambertian surfaces where the primary source of pixel variations within a composite cycle is associated with atmosphere contamination and path length, however, its major shortcoming is that the anisotropic, bi-directional influences of the surface is not considered. The bidirectional spectral behavior of numerous, 'global' land cover types and terrestrial surface conditions have been widely documented and shown to be highly anisotropic due to canopy structure, shadowing, and background contributions (Kimes et al., 1985; Leeuwen et al., 1994; Vierling et al., 1997). Ratioing of the NIR and red spectral bands to compute vegetation indices does not remove surface anisotropy (Walter-Shea et al., 1997) due to the spectral dependence of the BRDF response (Gutman, 1991; Roujean et al., 1992). The atmosphere counteracts and dampens the surface BRDF signal, mainly through the increasing path lengths associated with off-nadir view angles and/or sun angles. The maximum NDVI value selected is thus, related to both the bidirectional properties of the surface and the atmosphere, which renders the MVC-based selection unpredictable. The MVC favors cloud free pixels, but does not necessarily pick the pixel closest to nadir or with the least atmospheric contamination. Although the NDVI tends to increase for atmospherically corrected data, it does not mean that the highest NDVI is an indication of the best atmospheric correction. Many studies have shown the MVC approach to select off-nadir pixels with large, forward-scatter (more shaded) view angles and large solar zenith angles, which are not always cloud-free or atmosphere clear (Goward et al., 1991; Moody and Strahler, 1994; Cihlar et al., 1994b, 1997). This degrades the potential use of the VI for consistent and accurate comparisons of global vegetation types. The MVC method works best for data uncorrected for atmosphere, although numerous inconsistencies result (Gutman, 1991; Goward et al., 1991, 1994; Cihlar et al., 1994b, 1997). The MVC approach becomes less appropriate with atmospherically-corrected data sets, since the anisotropic behavior of surface reflectances and vegetation indices is stronger (Cihlar et al., 1994b). The influence of surface anisotropy and bidirectional reflectances on the VI composited products will become more pronounced in the EOS era as a result of improved atmospheric removal algorithms, which will accentuate differences and cause surface BRDF-related anisotropies to become more prominent (Cihlar et al.,1994a). In many cases, the nadir view direction may produce the lowest VI value, particularly in atmospherically corrected data.

There are other alternatives to simply choosing the highest NDVI value over a compositing cycle. One may integrate or average all cloud-free pixels over the period. Meyer et al. (1995) suggested that averaging the NDVI would be superior to the MVC approach. The Best Index Slope Extraction (BISE; Viovy et al., 1992) method reduces noise in NDVI time series by selecting against spurious high values through a sliding compositing cycle. Use of the thermal channel has also been shown to be helpful. Knowledge of the ecological evolution of a land cover with respect to a VI temporal response might also be of use for the improvement of compositing techniques (Viovy et al.,1992; Qi et al., 1994; Moody and Strahler, 1994). This was not considered for the MODIS compositing algorithm due to the amount of knowledge required of the dynamics of land cover growth patterns, seasonality, and response to climate change (precipitation, temperature). Such an approach might be more applicable at regional scales. Other VI compositing techniques are discussed by Cihlar et al. (1994b) and Qi and Kerr (1997). The global operational use of a vegetation index requires that it not only be calculated in a uniform manner, but that the results be comparable over time and location.

We propose to use MVC in the compositing the OCM-3 biophysical products.

Although the NDVI has been shown useful in change detection, land surface monitoring, and in estimating many biophysical vegetation parameters, there is a history of vegetation index research identifying limitations in the NDVI, which may impact upon its utility in global studies. These limitations form the basis of VI optimization techniques and are useful to

understand before utilization of the VI product. Limitations can result from various external influences such as:

· Calibration and instrument characteristics.
· Clouds and cloud shadows.
· Atmospheric effects due to variable aerosols, water vapor, and residual clouds.
· Sun-target-sensor geometric configurations and the resulting interactions of surface.
- Atmospheric anisotropies on the angular dependent signal.

In addition to these external influences, there are influences inherent to vegetated canopies which restrict the use and/or interpretation of vegetation indices. These include:

· Canopy background contamination in which the background reflected signal intimately mixes with the vegetation signal and influences the resulting VI value. Canopy background signals vary with soils, litter covers, snow, and surface wetness.

· Saturation problems whereby VI values remain invariant to changes in the amount, type, and condition of vegetation, normally associated with a saturated chlorophyll signal in densely vegetated canopies. Furthermore, if one were to extend VI capabilities to the derivation of biophysical vegetation parameters, then one must take into account the following:

· Canopy structural effects associated with leaf angle distributions, clumping and non-photosynthetically-active components (woody, senesced, and dead plant materials). Thus for a given LAI, %cover, and/ or biomass, the NDVI may vary with changes in the structure and orientation of the canopy. The 'strength' of the vegetation signal is simultaneously dependent upon several 'physical' measures of vegetation amount, including leaf area index, %green cover, and wet or dry green biomass.

· Non-linearity in VI relationships with fAPAR and/ or LAI.

Thus two vegetation indices namely NDVI and EVI will be generated from OCM-3 along with other biophysical parameter, VF using the proposed algorithm along with their composite by applying MVC method. Cloud pixel filtering will be a stringent requirement for our products and algorithms assume availability of cloud-free pixel observations. These three products will be quite useful for the purpose of global vegetation monitoring on regular basis for various applications.

Acknowledgements:
The author would like to thank Director, Space Applications Centre, ISRO for his encouragement and support to this study.

References

Agbu, P. A. and James, M. E. (1994), The NOAA/NASA Pathfinder AVHRR Land Data Set User's Manual. Goddard Distributed Active Archive Center, NASA, Goddard Space Flight Center, Greenbelt, MD.

Archard, F., Malingreau, J. P., Phulpin, T., Saint, G., Saugier, B., Seguin, B., and Vidal Madjar, D. (1994), A mission for global monitoring of the continental biosphere. VEGETATION International Users Committee Secretariat, Joint Research Centre, Institute for Remote Sensing Applications, I-21020 ISPRA (Va) Italy. http://www-vegetation.cst.cnes.fr:8050/.

Asrar, G., Fuchs, M., Kanemasu, E. T., and Hatfield, J. L. (1984), Estimating absorbed photosynthetic radiation and leaf area index from spectral reflectance in wheat, Agron. J., 76:300-306.

Baret, F. and Guyot, G. (1991), Potentials and limits of vegetation indices for LAI and APAR assessment, Remote Sens. Environ., 35:161-173.

Daughtry, C. S. T., Gallo, K. P., Goward, S. N., Prince, S. D., and Kustas, W. P. (1992), Spectral estimates of absorbed radiation and phytomass production in corn and soybean canopies, Remote Sens. Environ, 39:141-152.

Daughtry, C. S. T., Gallo, K. P., Goward, S. N., Prince, S. D., and Kustas, W. P. (1992), Spectral estimates of absorbed radiation and phytomass production in corn and soybean canopies, Remote Sens. Environ, 39:141-152.

Deering, D. W. (1978), Rangeland reflectance characteristics measured by aircraft and spacecraft sensors. Ph.D. Dissertation, Texas A & M University, College Station, TX, 338 pp.

Eidenshink, J. C. and Faundeen, J. L. (1994), The 1km AVHRR global land data set: first stages in implementation, Int. J. Remote Sensing, 15(17):3443-3462.

Fung, Y., Tucker, C. J. and Prentice, K. C. (1987), Application of Advanced Very High Resolution Radiometer vegetation index to study atmosphere-biosphere exchange of CO2, J. Geoph. Res., 92, 2999-3015.

Goward, D. G., Turner, S., Dye, D. G., and Liang, J. (1994), University of Maryland improved Global Vegetation Index, Int. J. Remote Sensing, 15(17):3365-3395.

Goward, S. N., Markham, B. L., Dye, D. G., Dulaney, W., and Yang, J. (1991), Normalized difference vegetation index measurements from the Advanced Very High Resolution Radiometer, Remote Sens. Environ., 35:257-277.

Gutman, G. (1991), Vegetation indices from AVHRR: an update and future prospects,Remote Sens. Environ., 35:121-136.

Holben, B. N. (1986), Characterization of maximum value composites from temporal AVHRR data, Int. J. Remote Sensing, 7:1417-1434.

Holben, B. N. (1986), Characterization of maximum value composites from temporal AVHRR data, Int. J. Remote Sensing, 7:1417-1434.

Hooker, S. B., Esaias, W. E., Feldman, G. C., Gregg, W. W., and McClain, C. R. (1992), An Overview of SeaWiFS and Ocean Color. NASA Tech. Memo. 04566, Vol. 1, S.B. Hooker and E.R. Firestone, Eds., NASA Goddard Space Flight Center, Greenbelt, Maryland, 24 pp.

Huete, A., Justice, C. and Liu, H. (1994), Development of vegetation and soil indices for MODIS-EOS, Remote Sens. Environ., 49:224-234.

James, M. D. and Kalluri, S. N. V. (1994), The Pathfinder AVHRR land data set: An improved coarse resolution data set for terrestrial monitoring, Int. J. Remote Sensing, 15(17):3347-3363.

Justice, C., Hall, D., Salomonson, V., Privette, J., Riggs, G., Strahler, A., Lucht, W., Myneni, R.,Knjazihhin, Y., Running, S., Nemani, R., Vermote, E., Townshend, J., Defries, R., Roy, D., Wan, Z.,Huete, A., van Leeuwen, W., Wolfe, R., Giglio, L., Muller, J-P., Lewis, P., and Barnsley, M. (1998), The Moderate Resolution Imaging Spectroradiometer (MODIS): Land remote sensing for global change research, IEEE Trans. Geosci. and Remote Sens., 36(4):1228-1249.

Justice, C., Hall, D., Salomonson, V., Privette, J., Riggs, G., Strahler, A., Lucht, W., Myneni, R.,Knjazihhin, Y., Running, S., Nemani, R., Vermote, E., Townshend, J., Defries, R., Roy, D., Wan, Z.,Huete, A., van Leeuwen, W., Wolfe, R., Giglio, L., Muller, J-P., Lewis, P., and Barnsley, M. (1998), The Moderate Resolution Imaging Spectroradiometer (MODIS): Land remote sensing for global change research, IEEE Trans. Geosci. and Remote Sens., 36(4):1228-1249.

Kaufman, Y. J. and Tanre, D. (1996), Strategy for direct and indirect methods for correcting the aerosol effect on remote sensing: from AVHRR to EOS-MODIS, Remote Sens. Environ., 55:65-79.

Kaufman, Y. J. and Tanre, D. (1996), Strategy for direct and indirect methods for correcting the aerosol effect on remote sensing: from AVHRR to EOS-MODIS, Remote Sens. Environ., 55:65-79.

Myneni, R. B, Keeling, C. D., Tucker, C. J., Asrar, G., and Nemani, R. R. (1997), Increased plant growth in the northern high latitudes from 1981 to 1991, Nature 386:698-702.

Myneni, R. B., Hall, F. G., Sellers, P. J., and Marshak, A. L. (1995), The interpretation of spectral vegetation indices, IEEE Trans. Geosci. Remote Sensing, 33(2):481- 486.

Myneni, R. B., Hall, F. G., Sellers, P. J., and Marshak, A. L. (1995), The interpretation of spectral vegetation indices, IEEE Trans. Geosci. Remote Sensing, 33(2):481- 486

Pinter, P. J., Jr. (1993), Solar angle independence in the relationship between absorbed PAR and remotely sensed data for alfalfa, Remote Sens. Environ, 46:19-25.
Prince, S. D., Justice, C. O., and Moore, B. (1994), Remote Sensing of NPP, IGBP DIS Working Paper #10, IGBP-DIS, Paris.
Prince, S. D., Kerr, Y. H., Goutorbe, J. P., Lebel, T., Tinga, A., Bessemoulin, P., Brouwer, J., Dolman, A. J., Engman, E. T., Gash, J. H. C., Hoepffner, M., Kabat, P., Monteny, B., Said, F., Sellers, P., and Wallace, J. (1995), Geographical, biological and remote sensing aspects of the Hydrologic Atmospheric Pilot Experiment in the Sahel (HAPEX-Sahel), Remote Sens. Environ., 51:215-234.
Raich, J. W. and Schlesinger, W. H. (1992), The global carbon dioxide flux in soil respiration and its relationship to vegetation and climate, Tellus, 44B:81-99.
Running, S. W. and Nemani, R. R. (1988), Relating seasonal patterns of the AVHRR vegetation index to simulated photosynthesis and transpiration of forest in different climates, Remote Sens. Environ., 24:347-367.
Sellers, P. J. (1985), Canopy reflectance, photosynthesis and transpiration, Int. J. Remote Sensing, 6:1335-1372.
Sellers, P. J., Tucker, C. J., Collatz, G. J., Los, S., Justice, C. O., Dazlich, D. A., and Randall, D. A. (1994), A global 1° * 1° NDVI data set for climate studies. Part 2 - The adjustment of the NDVI and generation of global fields of terrestrial biophysical parameters, Int. J. Remote Sensing, 15:3519-3545.
Tans, P. P., Fung, I. Y., and Takahashi, T. (1990), Observational constraints on the global atmosphere CO2 budget, Science, 247:1431-1438.
Townshend, J. R. G., Justice, C. O., Gurney, C., and McManus, J. (1992), The impact of misregistration on the detection of changes in land cover, IEEE Trans. Geosci. Remote Sens., 30(5):1054-1060.
Townshend, J. R. G., Justice, C. O., Skole, D., Malingreau, J. P., Cihlar, J., Teillet, P., Sadowski, F., and Ruttenberg, S. (1994), The 1 km resolution global data set: needs of the International Geosphere Biosphere Programme, Int. J. Remote Sensing, 15:3417-3441.
Vermote, E., El Saleous, N., Justice, C. O., Kaufman, Y. J., Privette, J. L., Remer, L., Roger, J. C., and Tanré, D. (1997b), Atmospheric correction of visible to middleinfrared EOS-MODIS data over land surfaces: background, operational algorithm and validation, J. Geoph. Res., 102(D14):17131-17141.
Vermote, E., Tanré, D., Deuzé, J. L., Herman, M., and Mocrette, J. J. (1997a), Second Simulation of the Satellite Signal in the Solar Spectrum (6S): an overview, IEEE Trans. Geosc. Remote Sens., 35(3):675-686.
Viovy, N., Arino, O., and Belward, A. S. (1992), The best index slope extraction (BISE): a method for reducing noise in NDVI time series, Int. J. Remote Sensing, 13:1585-1590.